Orbital Magnetism and Spin-Orbit Effects in the Electronic Structure of $BaIrO_3$

M. A. Laguna-Marco,[1,*] D. Haskel,[1,¶] N. Souza-Neto,[1] J. C. Lang,[1] V. V. Krishnamurthy,[2] S. Chikara,[3] G. Cao,[3] and M. van Veenendaal[1,4,‡]

[1]*Advanced Photon Source, Argonne National Laboratory, Argonne, Illinois 60439, USA*
[2]*Neutron Scattering Sciences Division, Oak Ridge National Laboratory, Oak Ridge, Tennessee 37831-6393, USA*
[3]*Department of Physics and Astronomy, University of Kentucky, Lexington, Kentucky 40506, USA*
[4]*Department of Physics, Northern Illinois University, De Kalb, Illinois 60115, USA*

(Received 3 June 2010; published 19 November 2010)

The electronic structure and magnetism of Ir $5d^5$ states in nonmetallic, weakly ferromagnetic $BaIrO_3$ are probed with x-ray absorption techniques. Contrary to expectation, the Ir $5d$ orbital moment is found to be $\sim$1.5 times larger than the spin moment. This unusual, atomiclike nature of the $5d$ moment is driven by a strong spin-orbit interaction in heavy Ir ions, as confirmed by the nonstatistical large branching ratio at Ir $L_{2,3}$ absorption edges. As a consequence, orbital interactions cannot be neglected when addressing the nature of magnetic ordering in $BaIrO_3$. The local moment behavior persists even as the metallic-paramagnetic phase boundary is approached with Sr doping or applied pressure.

DOI: 10.1103/PhysRevLett.105.216407 PACS numbers: 71.20.−b, 75.47.Lx, 75.50.Dd, 78.70.Dm

Recently, second ($4d$)- and third ($5d$)-row transition-metal oxides have generated significant excitement due to the observation of unexpected orbital ordering [1] and localized transport and magnetism [2,3] in ruthenate and iridate compounds, respectively. Since the spatial extent of the d electronic wave function increases for $3d \rightarrow 5d$, the electronic and magnetic properties of higher-row transition-metal ions would be expected to display itinerantlike behavior due to strong band effects. The concomitant decrease in Coulomb interactions would also disfavor the creation of local moments. However, it has been recently pointed out [2–4] that strong spin-orbit interactions can lead to an insulating and antiferromagnetic (I-AFM) state in iridates with half-filled ($5d^5$) Ir^{4+} ions even in the presence of weak electron correlations. In perovskitelike Sr_2IrO_4, large spin-orbit interactions within the t_{2g} manifold of the crystal-field-split $5d$ states result in effective total angular momentum $j_{\text{eff}} = \frac{1}{2}, \frac{3}{2}$ states ($l_{\text{eff}} = 1$; $s = \frac{1}{2}$) [2–4]. The $j_{\text{eff}} = \frac{1}{2}$ states close to the Fermi level form an effective single-band Hubbard model showing a gap due to weak electron-electron interactions leading to an I-AFM state [2,4]. By contrast, the perovskite $SrIrO_3$ is a paramagnetic metal [5].

The layered iridate $BaIrO_3$ also markedly departs from the canonical, band-driven itinerant picture. Its electrical resistivity was determined to be nonmetallic but on the verge of a metallic state [6,7]. In addition, it displays weak ferromagnetism with $\mu \approx 0.03\mu_B$/Ir, much smaller than expected for a ${}^2T_{2g}$ low-spin ($S = 1/2$) Ir^{+4} state and about one-third the size of the ferromagnetic moment in Sr_2IrO_4 [3]. This small moment was first explained in terms of canting of antiferromagnetically coupled, localized spin moments [8]. However, muon-spin resonance (μ-sR) studies [9], together with small values of the saturated moment (even at 30 T) and the effective moment in the paramagnetic state ($0.13\mu_B$/Ir), appear to best fit a description based on delocalized electrons, where the small Ir moment is due to $5d$-$2p$ hybridization and a small exchange splitting in the $5d$ bands [10,11]. Early tight-binding and local-spin-density approximation calculations support itinerant ferromagnetism within a Stoner picture [12,13]. Experimental evidence, however, including the observation of high coercivity and anisotropy in magnetization measurements, nonmetallicity, and the simultaneous onset of charge density wave formation at the magnetic ordering temperature [6,10], cannot be reconciled with a spin-only, itinerant picture of magnetism and suggest the existence of a more complex electronic ground state. In particular, the role of spin-orbit interactions, neglected in the theoretical calculations [12,13], has to be addressed experimentally.

In this Letter, x-ray absorption spectroscopy (XAS) and x-ray magnetic circular dichroism (XMCD) measurements demonstrate that a spin-only, itinerant description of the Ir $5d$ magnetism is incorrect. Sum rule analysis of XAS and XMCD signals reveals the presence of a strong spin-orbit coupling in the ground state and a larger orbital than spin contribution to the local magnetic moment. Detailed analysis of the XAS and XMCD line shapes using theoretical calculations show that band effects are not strong enough to destroy the local moments. The importance of orbital and spin interactions upon the magnetic ground state is also addressed.

Polycrystalline $BaIrO_3$ was synthesized using a solid-state reaction, whereas Sr doped samples ($Ba_{1-x}Sr_xIrO_3$, $x = 0.06$, 0.12) were grown as single crystals using the self-flux technique [6,10]. The XAS/XMCD measurements were carried out at the beam line 4-ID-D of the Advanced Photon Source, Argonne National Laboratory at the Ir $L_{2,3}$ absorption edges ($2p_{1/2,3/2} \rightarrow 5d$ transition). Circularly

polarized x rays were generated using a 500 μm-thick diamond (111) phase retarder [14,15]. XMCD was measured by switching x-ray helicity (12.7 Hz) and detecting the related modulation in the absorption coefficient with a lock-in amplifier [16]. Powder samples were measured in transmission on warming after field cooling in a magnetic field of 0.4 T applied along the x-ray propagation direction.

Figure 1 shows the Ir $L_{2,3}$-edge isotropic and circular dichroic x-ray absorption spectra of $Ba_{1-x}Sr_xIrO_3$ at $T = 5$ K for $x = 0, 0.06, 0.12$ samples. Surprisingly, strong "white lines" (shadowed area in Fig. 1) are observed at both absorption edges. This enhanced absorption is indicative of a large local density of $5d$ states. Additionally, the branching ratio $\mathrm{BR} = I_{L_3}/I_{L_2}$, where $I_{L_{2,3}}$ is the integrated white line intensity at a particular spin-orbit split edge, is close to 4 for the three compounds. This differs significantly from the statistical branching ratio of 2, characteristic of Ir metal [17], Ir alloys [17–19], or Ir-Fe multilayers [20]. The branching ratio is an important quantity, since it is directly related to the ground-state expectation value of the angular part of the spin-orbit coupling $\langle \mathbf{L} \cdot \mathbf{S} \rangle$ of $5d$ states via $\mathrm{BR} = (2 + r)/(1 - r)$, where $r = \langle \mathbf{L} \cdot \mathbf{S} \rangle / \langle n_h \rangle$ and n_h is the number of holes [21]. A strong deviation from 2 indicates the presence of a strong coupling between the local orbital and spin moments. Note that the branching ratio is sensitive to the ground-state expectation value $\langle \mathbf{L} \cdot \mathbf{S} \rangle$, and not to the spin-orbit interaction in the Hamiltonian, $H_{\mathrm{so}} = \zeta_{5d} \mathbf{L} \cdot \mathbf{S}$, itself ($\zeta_{5d}$ is the spin-orbit coupling constant). Even in the presence of a spin-orbit interaction the expectation value can be small if the moments are quenched. Obviously, this is not the case for

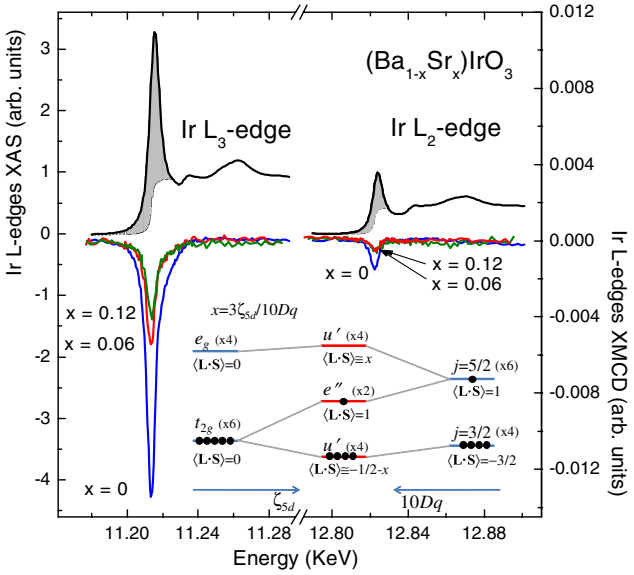

FIG. 1 (color online). XAS (left axis) and XMCD (right axis) spectra at the Ir $L_{2,3}$ edges for $Ba_{1-x}Sr_xIrO_3$. The inset shows a schematic energy diagram of how the d levels split under the influence of crystal-field and spin-orbit interactions.

$BaIrO_3$. Using $n_h \cong 5$ we obtain $\langle \mathbf{L} \cdot \mathbf{S} \rangle \cong 2$ in units of $\hbar^2$. The spin-orbit interaction splits the t_{2g} states into $j_{\mathrm{eff}} = \frac{3}{2}, \frac{1}{2}$ states. For a hole with $j_{\mathrm{eff}} = 1/2$, one expects a spin-orbit value of $\langle \mathbf{L} \cdot \mathbf{S} \rangle = -\frac{1}{2}[j_{\mathrm{eff}}(j_{\mathrm{eff}} + 1) - l_{\mathrm{eff}}(l_{\mathrm{eff}} + 1) - s(s + 1)]\rangle = 1$, noting that the angular momentum is opposite to the effective angular momentum ($\mathbf{L} = -\boldsymbol{l}_{\mathrm{eff}}$) [4]. The value of the spin-orbit coupling can also be understood from the fact that the $j_{\mathrm{eff}} = 1/2$ states originate from the splitting of the $j = 5/2$ states into e'' and u' under the influence of a crystal field; see the inset in Fig. 1.

In order to clarify the discrepancy with the experimental value, we have determined the branching ratio numerically using configuration interaction (CI) calculations for an Ir^{4+} ion [22]. Calculations have been done, including the spin-orbit interaction for the core and valence shells, Coulomb interaction, and an octahedral crystal field. Parameters are calculated using the Hartree-Fock approximation. In our calculation, we consider the total local moment given by the five $5d$ electrons. The ${}^2T_{2g}$ state in octahedral symmetry (no spin-orbit coupling) is split into twofold and fourfold degenerate states under the influence of the spin-orbit interaction (E'' and U' symmetries, respectively). For an E'' ground state ($u'^4 e''$), the L_3/L_2 branching ratio can be reproduced with a spin-orbit coupling parameter of $\zeta_{5d} = 0.3$ eV ($n_h = 5$), where ζ_{5d} has been reduced from its atomic value by 25% to account for band effects. The corresponding $\langle \mathbf{L} \cdot \mathbf{S} \rangle$ is 2.1. We can distinguish two contributions to $\langle \mathbf{L} \cdot \mathbf{S} \rangle$. The direct term from the e'' ($j_{\mathrm{eff}} = 1/2$) states explains about half of the value. The remainder of $\langle \mathbf{L} \cdot \mathbf{S} \rangle$ comes from the mixing by the spin-orbit interactions of the u' terms from the t_{2g} (or $j = 3/2$) states with the states of the same symmetry arising from the e_g (or $j = 5/2$) states. This indirect term is of the order of $\zeta_{5d}/10Dq$. This coupling more than doubles the value of $\langle \mathbf{L} \cdot \mathbf{S} \rangle$, giving 2.1, in agreement with experiment. It also indicates that the spin-orbit coupling mixes e_g and t_{2g} orbitals in the ground state.

The spectral line shape is shown in detail in Fig. 2. Since the ground state of Ir^{4+} is, to lowest order, low spin, t_{2g}^5, excitations can be made into the empty t_{2g} and e_g states. The isotropic spectrum shows both components. However, the dichroism mainly occurs in the t_{2g}-derived states, leading to a shift towards lower energy of the XMCD proportional to the crystal-field splitting $10Dq$; see Fig. 2(a). We can derive an effective crystal field of $10Dq = 2.9$ eV. Calculations for $10Dq = 2.5$ and 3.3 eV clearly do not reproduce the shift of the XMCD with respect to the XAS.

Another important factor that can affect the branching ratio is whether band effects are sufficiently strong to mix the E'' ($u'^4 e''$) and U' ($u'^3 e''^2$) symmetries that locally arise from the splitting of the ${}^2T_{2g}$ state due to the $5d$ spin-orbit interaction. Figure 2(b) shows the effect on the spectral line shape when 10% and 28% U' is mixed into the ground state. Although the isotropic spectrum looks satisfactory,

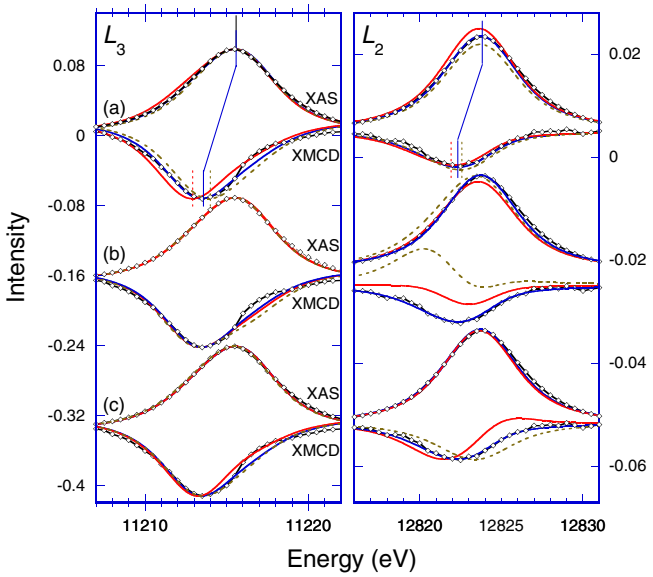

FIG. 2 (color online). Comparison between XAS and XMCD experimental data (dotted lines) and numerical calculations for $BaIrO_3$ (XMCD is scaled to the XAS). (a) Dependence of the spectral line shape on the crystal field with $10Dq = 2.5$ (brown dashed line), 2.9 (blue line), and 3.3 (red line). (b) Effect of mixing of E'' and U' ground-state symmetries (approximately $j_{\text{eff}} = 1/2$ and $3/2$ states) with 0% (blue line), 10% (red line), and 22% (brown dashed line) U' component in the ground state. (c) Effect of the effective exchange field: pure S_z (red line), pure L_z (brown dashed line), and proportional to $L_z + 5S_z$ (blue line).

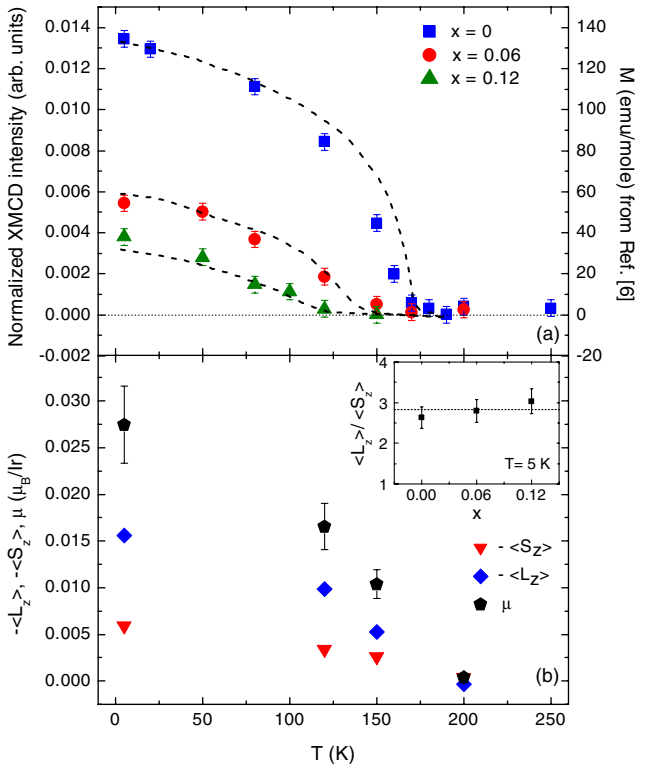

FIG. 3 (color online). (a) Thermal dependence of XMCD intensity at the Ir L_3 edge (left axis) and magnetization data [6]. (b) Ground-state expectation values of L_z, S_z, and the magnetic moment $\mu = -(\langle L_z\rangle + 2\langle S_z\rangle)$ of $BaIrO_3$ as a function of temperature. Inset: $\langle L_z\rangle/\langle S_z\rangle$ ratio for several Sr dopings.

discrepancies occur in the XMCD. The XMCD at the L_2 edge decreases significantly for 10% and changes sign for 28% U' character in the ground state. Hence, we can conclude that the local E'' ground state is pure and that no significant mixing between the different symmetries takes place.

XMCD sum rules, $(I^c_{L_3} - 2I^c_{L_2})/(I^c_{L_3} + I^c_{L_2}) = (4\langle S_z\rangle + 14\langle T_z\rangle)/(3\langle L_z\rangle)$, are used to obtain information on the ground-state expectation values of L_z and S_z [23,24]. Here $I^c_{L_{2,3}}$ are experimental XMCD intensities, and T_z is the magnetic dipole moment. Using $14\langle T_z\rangle/4\langle S_z\rangle = 0.64$ obtained from the CI calculations, we find a ratio $\langle L_z\rangle/\langle S_z\rangle = 2.8(2)$. The neglect of T_z, as is often done, would underestimate this ratio, giving $\langle L_z\rangle/\langle S_z\rangle = 1.8$. The ordered magnetic moment obtained from sum rules ($0.027\,\mu_B$/Ir at $T = 5$ K and $H = 0.4$ T) and the magnetic ordering temperatures are in very good agreement with values from magnetization measurements [6] (see Fig. 3). Clearly, the orbital moment dominates the magnetic moment. The equal signs of $\langle L_z\rangle$ and $\langle S_z\rangle$ are not in contradiction with a $j_{\text{eff}} = 1/2$ state, since the real moment is opposite to the effective moment, $\mathbf{L} = -\boldsymbol{l}_{\text{eff}}$. The values for a single hole in the $j_{\text{eff}} = 1/2$ state are $\langle L_z\rangle = -2/3, \langle S_z\rangle = -1/6$, giving a ratio of 4 [4]. Considering the total t^5_{2g} moment does not significantly affect this value. An incoherent mixture of the two components of the E'' local symmetry due to band effects would not directly affect the branching ratio. However, the ratio can be reduced by considering an effective exchange field $H_{\text{exch}} = \alpha L_z + \beta S_z$. While in most transition-metal compounds the spectral line shape is rather insensitive to the specific nature of H_{exch}, the iridium system shows a remarkable sensitivity; see Fig. 2(c). If the spins only interact via a (symmetric) superexchange interaction, i.e. $\alpha = 0$, there is a clear discrepancy between theory and experiment. Similarly, a pure orbital interaction ($\beta = 0$) yields a clear shift to higher energies. The best agreement is obtained for $H_{\text{exch}} \sim L_z + 5S_z$, which increases the local orbital and spin moments by ~40 and 80%, respectively, but reduces the ratio to the experimental value of 2.8. This clearly indicates the complexity of the magnetic interactions in $BaIrO_3$.

It is informative to make a comparison with $4d$ transition-metal compounds, where angle-resolved photoemission and density functional theory [2,25–27] also claim the presence of strong spin-orbit coupling effects. Experimentally, however, the isotropic BR in ruthenium and rhodium compounds is close to the statistical value of 2 [28–30]. The coupling between the spin and orbital moments in the $4d$ series is therefore relatively weak. Similarly, the XMCD spectra at the $L_{2,3}$ edges of Ru in $Ca_{1-x}Sr_xRuO_3$ [29] are almost equal in magnitude and opposite in sign, indicating a very small orbital moment

in the 4*d* states [23]. This is also observed in Ir metallic alloys and heterostructures, where a 5*d* Ir spin moment is induced by hybridization with, or in proximity to, spin-polarized orbitals of other transition metals [18–20]. In contrast our XMCD signals have equal signs at both $L_{2,3}$ edges, and the L_2-edge peak intensity is 9.6 times smaller than the L_3 edge. This indicates a sizable orbital moment in the 5*d* states of $BaIrO_3$.

Finally, let us consider the dependence of the local moment on temperature and bandwidth. The ordered Ir 5*d* moment is decomposed into orbital and spin parts in Fig. 3(b). Although the ordered moment probed by XMCD is reduced with temperature, the orbital-to-spin moment ratio is not reduced since the local moment is preserved. Similarly, we can probe the effect of the bandwidth by the application of chemical pressure (substitution of Ba^{2+} by Sr^{2+} ions) or external pressure. Sr doping reduces the ordered moment [Fig. 3(a)] but the local moment is stable, as seen from the constant L_z/S_z ratio in the inset of Fig. 3(b). The same behavior is noted when applying external pressure to $BaIrO_3$, which causes the disappearance of magnetic ordering at $P \sim 4.5(5)$ GPa but preserves the local moment and the L_z/S_z ratio [31]. While band broadening reduces the strength of exchange interactions and suppresses magnetic ordering, the robustness of the L_z/S_z ratio is consistent with the sizable spin-orbit coupling of about 0.3 eV, an order of magnitude larger than exchange interactions ($T_c \sim 175$ K). It is likely that the loss of magnetism with external pressure is accompanied by a transition into a metallic state, as observed with Sr doping, which would be another indication of the delicate interplay between electronic bandwidth, Coulomb, and spin-orbit interactions in this spin-orbit driven system. This, however, would have to be confirmed by direct transport or optical conductivity measurements under pressure.

In summary, whereas XAS and XMCD measurements on (3*d*, 4*d*) materials show nearly statistical isotropic branching ratios and small orbital/spin moment ratios, the stronger spin-orbit coupling in 5*d* transition-metal oxides dominates the electronic properties and leads to a nearly pure E'' ($u'^4 e''$) ground state in $BaIrO_3$, even in the presence of band effects. The ground state is more complex than expected for a model including only the t_{2g} states [3,4]. The local moments couple through both orbital and spin interactions, so structural details are bound to strongly influence the strength and nature of magnetic ordering. Apart from the presence of a strong crystal field, the physics of 5*d* compounds appears to have a remarkable similarity with actinide systems, where experiments show [32] that strong spin-orbit effects persist even in the presence of 5*f* electron delocalization.

Work at Argonne is supported by the U.S. Department of Energy (DOE), Office of Science, Office of Basic Energy Sciences, under Contract No. DE-AC-02-06CH11357. M. A. L.-M. acknowledges the Spanish MEC for a post-doctoral grant. M. v. V. was supported by the U.S. Department of Energy (DOE), Office of Basic Energy Sciences, Division of Materials Sciences and Engineering, under Grant No. DE-FG02-03ER46097. S. C. and G. C. were supported by NSF through Grants No. DMR-0552267 and No. DMR-0856234.

*laguna@icmm.csic.es
¶haskel@aps.anl.gov
‡veenendaal@niu.edu

[1] S. A. J. Kimber *et al.*, Phys. Rev. Lett. **102**, 046409 (2009).
[2] B. J. Kim *et al.*, Phys. Rev. Lett. **101**, 076402 (2008).
[3] B. J. Kim *et al.*, Science **323**, 1329 (2009).
[4] G. Jackeli and G. Khaliullin, Phys. Rev. Lett. **102**, 017205 (2009).
[5] S. J. Moon *et al.*, Phys. Rev. Lett. **101**, 226402 (2008).
[6] G. Cao, X. N. Lin, S. Chikara, V. Durairaj, and E. Elhami, Phys. Rev. B **69**, 174418 (2004).
[7] T. Nakano and I. Terasaki, Phys. Rev. B **73**, 195106 (2006).
[8] R. Lindsay, W. Strange, B. L. Chamberland, and R. O. Moyer, Jr., Solid State Commun. **86**, 759 (1993).
[9] M. L. Brooks *et al.*, Phys. Rev. B **71**, 220411(R) (2005).
[10] G. Cao *et al.*, Solid State Commun. **113**, 657 (2000).
[11] A. V. Powell and P. D. Battle, J. Alloys Compd. **191**, 313 (1993).
[12] M. H. Whangbo and H. J. Koo, Solid State Commun. **118**, 491 (2001).
[13] K. Maiti, Phys. Rev. B **73**, 115119 (2006).
[14] K. Hirano *et al.*, Jpn. J. Appl. Phys. **30**, L407 (1991).
[15] J. C. Lang and G. Srajer, Rev. Sci. Instrum. **66**, 1540 (1995).
[16] M. Suzuki *et al.*, Jpn. J. Appl. Phys. **37**, L1488 (1998).
[17] Y. Jeon, B. Qi, F. Lu, and M. Croft, Phys. Rev. B **40**, 1538 (1989).
[18] V. V. Krishnamurthy *et al.*, Hyperfine Interact. **136–137**, 361 (2001).
[19] G. Schütz *et al.*, Z. Phys. B **75**, 495 (1989).
[20] F. Wilhelm *et al.*, Phys. Rev. Lett. **87**, 207202 (2001).
[21] G. van der Laan and B. T. Thole, Phys. Rev. Lett. **60**, 1977 (1988).
[22] B. T. Thole *et al.*, Phys. Rev. B **32**, 5107 (1985).
[23] B. T. Thole, P. Carra, F. Sette, and G. van der Laan, Phys. Rev. Lett. **68**, 1943 (1992).
[24] P. Carra, B. T. Thole, M. Altarelli, and X. Wang, Phys. Rev. Lett. **70**, 694 (1993).
[25] T. E. Kidd *et al.*, Phys. Rev. Lett. **94**, 107003 (2005).
[26] F. Baumberger *et al.*, Phys. Rev. Lett. **96**, 246402 (2006).
[27] M. W. Haverkort *et al.*, Phys. Rev. Lett. **101**, 026406 (2008).
[28] Z. Hu *et al.*, Phys. Rev. B **61**, 5262 (2000).
[29] J. Okamoto *et al.*, Phys. Rev. B **76**, 184441 (2007).
[30] T. Burnus *et al.*, Phys. Rev. B **77**, 205111 (2008).
[31] M. A. Laguna-Marco *et al.* (to be published).
[32] K. T. Moore *et al.*, Phys. Rev. B **76**, 073105 (2007).